Highlights

A simple 2D numerical model is introduced to evaluate piezoelectric fan operation in a channel flow application

The model is validated using an approach derived from published literature

Performance of two adjacent piezoelectric fan blades is evaluated as the phase of oscillation between the blades is varied

Counter-phase is found to provide optimum performance, whilst low phase variation is shown to induce skewness to the downstream air velocity profile

Optimisation of Low Energy Cooling through Phase Variation between Adjacent Piezoelectric Fan Blades

Alastair Hales*, Xi Jiang

Abstract—Piezoelectric fans are highly efficient and low energy air-movers. The technology may be applied to reduce the power requirements of thermal management systems in a range of power electronics. The understanding of piezoelectric fan arrays, in which multiple blades are beneficially coupled, is of paramount importance for the research field. In the present research, a numerical model consisting of two piezoelectric fan blades is developed and validated against previous experimental work. The model is used to investigate the effect of phase variation, ϕ, between two adjacent piezoelectric fan blades in face-to-face orientation, operating within a channel. When $\phi \neq 0°$,180°, an asymmetrical flow domain is observed. Considering an incremental increase of phase variation from $\phi = 0°$, the skewness of the downstream velocity profile is increased heavily when $\phi \leq 60°$, whilst the magnitude of the average downstream velocity is only enhanced when $\phi \geq 75°$. The generated skew is attributed to the dominance of one vortex over another between the adjacent blade faces during their opening period. At peak skewness ($\phi = 75°$), the vortex behind the phase leading blade is 101% larger than its counterpart. Evenly matched vortices between the two blades are optimal for generating peak mass transfer. This is observed when the blades are in counter-phase, $\phi = 180°$. Conclusions in the present study build upon and are in good agreement with those previously published.

Keywords—Piezoelectric fans, low energy cooling, power electronics, computational fluid dynamics.

I. Introduction

Piezoelectric (PE) fans were first developed by Toda *et al.* [1], cited to be an ideal hotspot-cooling solution. A PE fan is a very low powered air-mover [2], and therefore ideal for placing inside small electronic assemblies to enhance convective heat transfer from heat sources. A PE fan is fabricated from a lead ziconate titanate (PZT) actuator, a blade and a clamp [3]. The actuator resonates the blade at high amplitude, approximately 10% of the blade length and dependent on driving power as well as geometric parameters, and high frequency, typically between 40 Hz and 100 Hz and determined by geometric parameters [4]. The blade tip generates vortices as it moves through the surrounding air [5] [6], equating to significant turbulence in the near vicinity of the blade tip which is harnessed in many applications to enhance mass and heat transfer from nearby heat sources [7] [2]. The fully grown vortex is detached from the blade tip as it reaches the edge of the oscillation envelope, due to the loss in pressure gradient between the leading and trailing blade face during deceleration [8] [9]. The subsequent motion of the blade tip, towards the centre of oscillation, drives the vortex downstream and this forms the basis of downstream airflow [10].

It is essential to consider system integration when evaluating PE fan performance in application. Work published by Hajmohammadi *et al.* analyses the performance of microchannel heat sinks [11], which are commonly allied with PE fans in operation to make use of the driven convective air flow to enhance the rate of heat transfer from small electrical components.

PE fans are highly efficient: in terms of heat transfer enhancement provided compared to power demanded, single PE fans outperform conventional axial fans by at least 100% [12] [13]. However, electronics systems' power densities have increased enormously in recent decades [14] [15] [16], and the heat they generate has increased in proportion [17] [18]. It is evident that PE fans, operating as a single unit, do not provide a feasible thermal management solution for many modern day applications. Air cooling, which for instance is used in 95% of ICT hardware in the present day [19], is almost always provided by small axial fans, which are capable of generating a large amount of airflow from a very small device [20] [21]. The methods and processes by which PE fan technology is used for applications must be developed in order to provide a feasible thermal management solution.

A. Piezoelectric Fan Arrays

PE fan arrays may provide a solution to increase the technology's relevance as a viable alternative air-mover [2]. PE fan arrays were first considered by Ihara and Watanabe [9], who demonstrated that two fan blades, orientated face-to-face (FTF) and oscillating in-phase with one another were able to generate greater than double the downstream volume airflow than a single PE fan operating alone. This initiated considerable subsequent research focussing on FTF arrays [22] [23] [24] [25], which are widely considered to be superior to those orientated edge-to-edge (ETE)[26]. As a consequence, certain optimal dimensionless parameters have been established.

A. Hales is with the Faculty of Engineering, Imperial College, South Kensington Campus, Exhibition Road, London, SW7 2AZ, UK; e-mail: a.hales@imperial.ac.uk .

X. Jiang is with the School of Engineering and Materials Science, Queen Mary University of London.

Manuscript received April 11th, 2019

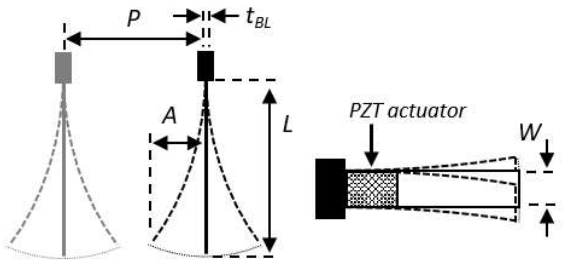

Fig. 1. Geometric parameters of piezoelectric fan and a fan blade array with face-to-face orientation

Pitch, P, the distance between two adjacent blade faces, has been highlighted as the key variable affecting array performance, and is most conveniently given as a function of oscillation amplitude, A [27]. A schematic of a two-blade array in FTF orientation is shown in Figure 1. The degree of coupling between the vortices generated from each blade is at a minimum for in-phase (IP) oscillation and increases to a maximum when adjacent blades are in counter-phase (CP) [25].

The vast majority of array based research focussing on airflow generation has been conducted in unconfined conditions, where side wall effects are negligable. At low pitch, $P \leq 4A$, the interaction between counter-rotating vortices during CP oscillation induces sigificant adverse flow between the blades [28] [29]. Additionally, the vortices generated during the opening period of CP oscillation are unable to grow to full size, and do not perform optimially as a result [25]. At low pitch but with IP oscillation, the vortices are better able to reach full size, 3-4A [25], rendering this phase superior [9] [29].

Above P=4A, the detrimental coupling associated with CP oscillation is reduced, and the benefits of two fully grown, counter-rotating vortices may be observed, where they are able to drive one another downstream [28]. Meanwhile, detrimental coupling becomes apparent with IP oscillation. Figure 2 shows the velocity profiles generated from a single blade and from a two-blade array, at P=8A, IP and in CP. It is evident that CP oscillation generates the greatest downstream air velocity per blade of the three cases, and IP oscillation is outperformed even by the single blade considering the same measure.

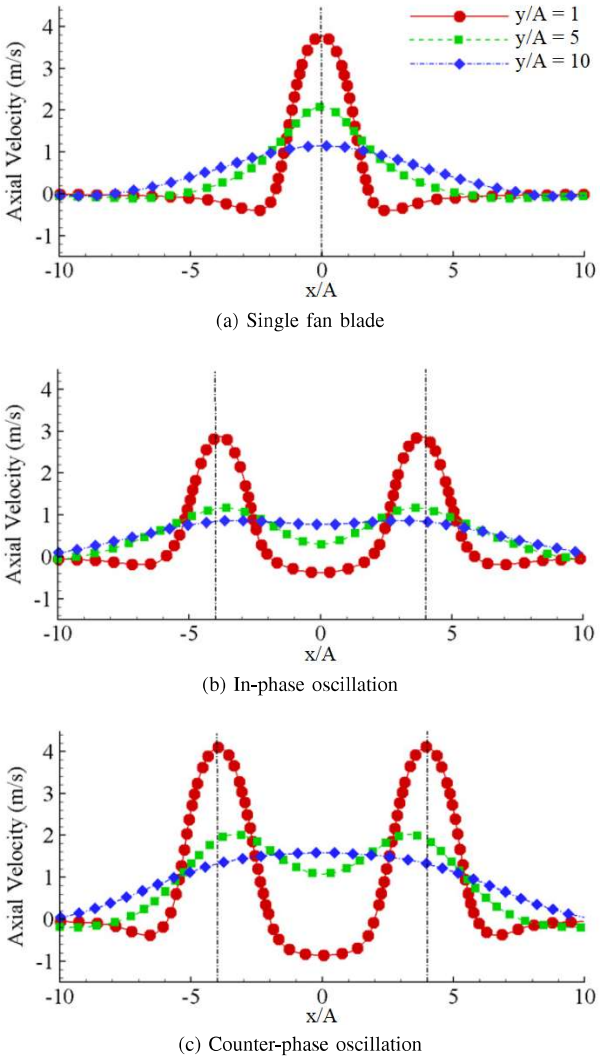

(a) Single fan blade

(b) In-phase oscillation

(c) Counter-phase oscillation

Fig. 2. Velocity profile of the downstream airflow at three distances downstream of oscillating fan blades [28]

B. Confined Piezoelectric Fan Arrays

Unconfined conditions are unrealistic for applications in power electronics, where space is at a premium [30]. Performance of heat sinks operating within a forced convection flow inside a channel is highly dependent on the aspect ratio of the microchannels embedded within the heat sinks [31]. In order to evaluate the performance of such heat sinks when used alongside a PE fan array, the performance, in terms of generated airflow from the PE fan array, must be thoroughly evaluated.

Kim *et al.* [32] experimentally investigated a channel flow situation with a single PE fan blade, where the blade was closely confined above and below it's edges, as shown in Figure 3. It was found that air was unable to freely flow around the blade edges during oscillation, from the leading to trailing faces.

Eastman and Kimber [33] [34] and Stafford and Jeffers [35] considered the effects of variable confinement on a single blade's faces and edges, and produced conflicting results [2]. The former concluded that airflow generation is unaffected by side wall proximity to the blade's edges, and is solely affected by confinement of the blade's faces. The latter argued that any blade confinement was highly detrimental to performance, and is capable of reducing airflow generation to just 20% of the optimum.

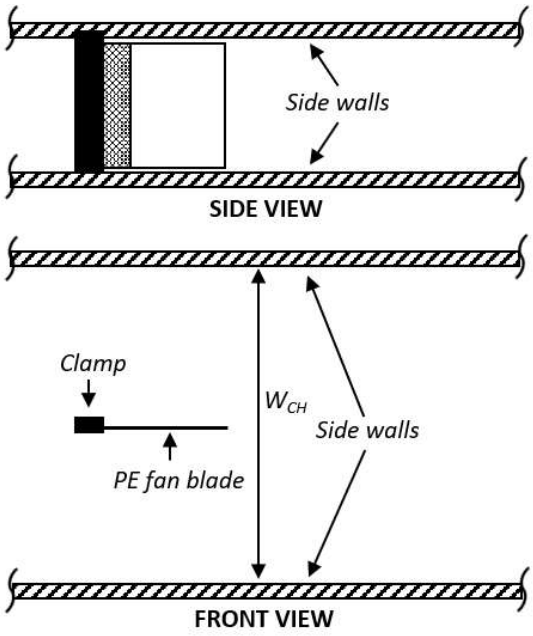

Fig. 3. Geometry and layout of the experimental channel flow equipment used by Kim *et al.* [32]

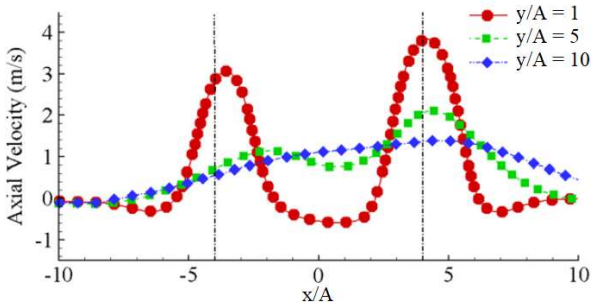

Fig. 4. Velocity profile of the downstream airflow at three distances downstream of oscillating fan blades, 90°out-of-phase [28]

C. Phase Variation

The instances in an oscillation cycle are described in terms of θ°. θ=0°occurs at the point instance the left-hand (LH) blade reaches its centre of oscillation, moving with a negative x-velocity. The right-hand (RH) blade instantaneous position is not described in terms of θ, but in terms ϕ°discrepancy from the LH blade. For instance, ϕ=0°for IP oscillation and ϕ=180°for CP oscillation.

The difference in phase, ϕ, between two adjacent blades in a FTF array, away from IP and CP has only been considered sparingly, and usually to a limited extent. Choi *et al.* [28] reported on a two-blade array in a channel flow environment with P=8A, oscillating at ϕ=0°, 45°, 90°, 135°and 180°. The time-averaged downstream velocity profile for the case ϕ=90°is displayed in Figure 4 where asymmetry is apparent.

It is stated that asymmetry is maximised at ϕ=90°, and the causes of the effect are a focus of Choi *et al.*'s investigation

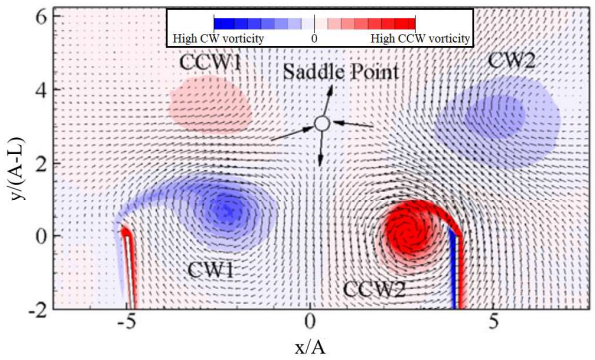

Fig. 5. Instantaneous velocity vector field and vorticity contour plot at θ=90°, for a two-blade array with ϕ=90°[28]

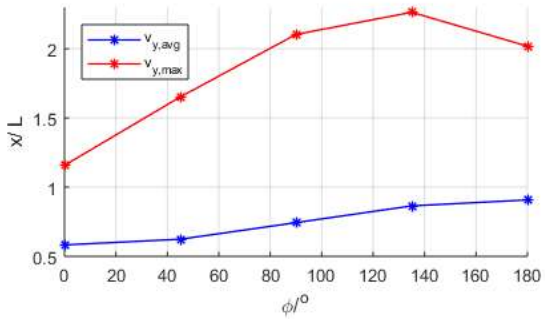

Fig. 6. Average and maximum time-averaged downstream velocities at y=L+ 5A for all reported cases of ϕ variance [28]

[28]. A velocity vector field of the relevant region is provided in Figure 5 for the instance at which the RH blade reaches the centre of oscillation (moving with a positive x-velocity) and the LH blade is stationary at the LH edge of its oscillation envelope, θ=90°. The asymmetric velocity profile is initially created by strong interaction between counter-rotating vortices CW1 and CCW2. The interaction initially inhibits CCW2's downstream propagation but CW1 is severely weakened as the RH blade begins to move with a negative x-velocity but the LH blade continues with a positive x-velocity (180< θ <270). The consequence is a weighting of airflow in the x >0 region.

Performance of two-blade arrays with varying ϕ, in terms of average and maximum time-averaged downstream air velocity ($v_{y,avg}$ and $v_{y,max}$) at y=L+5A, is presented in Figure 6 [28]. By both measures, IP oscillation performs worst. It is interesting to note that whilst CP oscillation optimised $v_{y,avg}$, which is proportional to downstream volume flow rate, ϕ=135°was preferable in terms of $v_{y,max}$. Airflow performance was not the focus of the discussed investigation [28]. Further evaluation of ϕ's relationship with the generated downstream airflow will resolve the existing knowledge gap in the field, and allow phenomena such as the one considered at ϕ=135°to be optimised for application.

D. Numerical Modelling of Piezoelectric Fans

As with other thermal management topics, numerical modelling is an essential component of research in the PE fan field [36]. Most often, modelling is carried out in a 3D domain [37] [38], because of the cruciality blade edge effects which 2D modelling neglects [39] [40]. The case of channel flow is unique however: blade edge effects are reduced as air is unable to move from the leading to trailing edge [34] [33]. As a result, modelling channel flow in 2D has been justified [8] [41] [2].

The focus of research is upon airflow, and therefore the energy equation may be eliminated as buoyancy effects are negligible without a heat source [12] [42]. Additionally, insubstantial pressure gradient allow incompressibility to be assumed [41], even in specific cases of confinement [43]. The same methodology has been applied by Choi *et al.* [8] [28], who were investigating PE fan performance under similar channel flow confinement. The inclusion of a second order discretisation term is becoming increasingly common as the computational capacity of hardware improves [39] [37].

Turbulent viscosity has been approximated through the SST k-ω model [44] [38] [45], RNG k-ε model [39] and LES model [46] in relevant literature. Very high turbulence may be optimally modelled with the standard k-ε model [47]. Choi *et al.* [8] [28] highlight the models strong performance with direct reference to the velocity profiles and vortices generated from an oscillating cantilever beam modelled in a 2D domain.

A PE fan blade may be defined as a simple clamped cantilever beam through Equation 1, where L and A_{XC} are the length and cross-sectional area of the defined blade ($W \cdot t_{BL}$) [48]. Maximum deflection, X, is determined for a point at distance y along the beam. The β coefficient may be derived through Equation 2 [48]. E, I, m and f_r define the blade material's Young's modulus and the blade's second moment of area, mass and oscillation frequency respectively.

$$\begin{aligned} X(y) = A_{XC} \cdot \big[\big(sin(\beta \cdot L) - sinh(\beta \cdot L)\big) \cdot \\ \big((sin(\beta \cdot y) - sinh(\beta \cdot y)\big) + \\ \big(cos(\beta \cdot L) - cosh(\beta \cdot L)\big) \cdot \\ \big((cos(\beta \cdot y) - cosh(\beta \cdot y)\big)\big] \end{aligned} \tag{1}$$

$$\beta = \sqrt[4]{\frac{2\pi \cdot f_r \cdot m}{L \cdot I \cdot E}} \tag{2}$$

Deflection in the PZT actuator region is limited, and this affects the blade shape [38]. Experimentally derived empirical functions, such as in Equation 3 [12], may be used to improve the mode shape definition. In this form, the function is only applicable to a blade of length 65 mm and a coefficient is necessary for global use.

$$\begin{aligned} X_{L65}(y_{L65}) = -42.3402 \cdot y_{L65}^2 + 33587.5 \cdot y_{L65}^3 \\ -2.7317 \cdot 10^6 \cdot y_{L65}^4 + 9.05342 \cdot 10^7 \cdot y_{L65}^5 \\ -1.2653 \cdot 10^9 \cdot y_{L65}^6 + 6.34496 \cdot 10^9 \cdot y_{L65}^7 \end{aligned} \tag{3}$$

Equation 4 defines the transient motion of the blade's nodes in a model, where x is the displacement from oscillation centre at time, t. Magnitude of power input is defined by the dimensionless coefficient D_c.

$$x(y,t) = D_c \cdot X(y) \cdot sin(2\pi \cdot f_r \cdot t) \tag{4}$$

The moving boundary is accomodated using a dynamic mesh [8]. In 2D, triangular elements are best suited to skewing and re-meshing, as they are able to remesh with a minimised change to the individual elements' centres of volume and volumetric size [8] [39]. The number of blade boundary oscillations completed is an important model parameter, and should be determined through preliminary computations assessing a certain outputted parameter. The quality of this computation is highly important, and discussed along with the experimental validation below. Achieving a repetitive state may require as many as 100 completed blade oscillations [37] [45] [26], or may be occur in as few as 20 [38] [39]. Across the relevant literature, a minimum of 100 time steps per oscillation is reported [37] [26]. In cases, the resolved solution has been improved by increasing this value [46] [49].

To validate a model, quantitative parameters within a solution must be compared to relevant experimental results. Basic validation of 2D or 3D models is achieved by comparing geometrically dependent outputs, most commonly system heat transfer coefficients. Reported error values range from 8% [10] to 17% [4] [37]. Hales and Jiang [2] highlight the limitations of such a process: it considers the effects of airflow, rather than the fundamental airflow parameters, and therefore a numerical model cannot be globalised (varying geometric or operational parameters) without further validation. Choi *et al.* [8] [28] [32] delivered validation of their numerical model by quantitatively comparing computationally derived airflow properties: downstream velocity profile, and vortex trajectory and size variation with those recorded from geometrically identical experimental set ups. As a result, they were evaluating the performance of their model against fundamental airflow characteristics, not coefficients conceived as a consequence of a particular experimental set up. For instance, it is reasonable to assume that two identical vortices will generate equal surface heat transfer coefficients from two identical surfaces, but it is unreasonable to assume that two equal heat transfer coefficients were a consequence of two identical vortices. The fundamental and quantitative validation therefore facilitates a greater degree of model parameter variation, without the need to revalidate computed results for every unique case [2].

E. Aims and Objectives

At present there is a considerable shortfall in the understanding of the effect of phase variation between two adjacent PE

fans: comparisons between oscillation phases in PE fan research are almost exclusively limited to IP and CP cases. As a consequence, phase is not considered a parameter that may be optimised in PE applications. This may be justifiable for cases of PE fan array use in free space, where IP oscillation is established to drive the greatest volume of air downstream. However, PE fans are increasingly being considered for operation in confined spaces, and therefore array the understanding of operation and optimisation for these applications must be developed. Published literature has presented numerical results for a specific case of channel flow confinement, where CP oscillation outperforms IP oscillation.

The primary aim of this study is to develop upon these initial findings and evaluate the performance of two adjacent PE fan blades operating with a range of phase variations. It is hypothesised, with validity from published literature, that unique asymmetric time-averaged downstream velocity profiles exist for the $\phi \neq 0°$, 180°cases. Two key parameters will be investigated, generated downstream airflow and airflow skewness. Skewing airflow, i.e. driving air in a direction misaligned with the downstream direction, may be essential for future PE fan array applications: optimal cooling may be focusable on different components within an assembly be varying the phase at which adjacent blades operate. Secondarily, computed results will develop understanding of the performance enhancement achieved through enabling CP oscillation, as opposed to IP.

Model validation is intrinsic to all aspects of the present study, and will be discussed in order to introduce methodology which may be further developed in future work in the field. The aim of the numerical model is firstly to be valid for a range of geometric domain characteristics, and secondly to computationally undemanding. Given the unique case of channel flow under investigation, a two-dimensional will be sufficient, as has been observed in published literature.

II. Methodology

A 2D numerical model, justifiable for the channel flow case under consideration, was located on the blade mid-span plane. As with all relevant literature, several assumptions we made in order to derive the presented model. The SIMPLE scheme was used to define pressure-velocity coupling and incompressibility was assumed. The energy equation, which had a very limited influence on the models resolution due to the lack of thermal gradients, was negated from the computation along with buoyancy considerations: it was assumed thermal and pressure gradients would be insignificant compared to other analysed aspects of the flow domain. The standard $k - \varepsilon$ model was used to define turbulence. The model was chosen based on strong results reported in the literature through its use [8] [28], and high levels of model validation, which is summarised in Section II-C.

The transient solution was formulated using a first order accurate implicit method, but a second order accurate upwind method of discretisation was employed to reduce model error. Convergence was monitored via residuals of five coefficients: x and y velocity, k, ε and continuity, and each was deemed sufficient when $\leq 10^{-4}$.

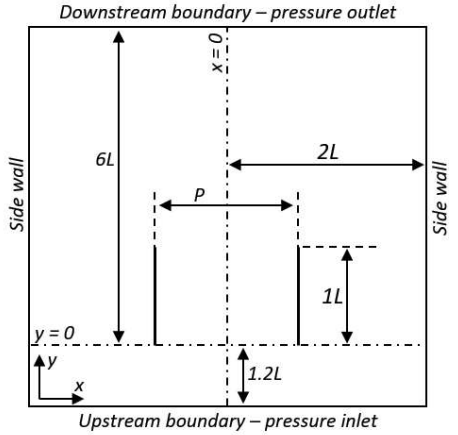

Fig. 7. Numerical domain used for the present investigation

A. Domain and Boundary Conditions

The domain geometry used is displayed in Figure 7. A two-blade array was preferred to assess the effects of ϕ variation because the introduction of further blades was shown to induce additional vortex interactions and would have complicated analysis of the key variable. Preliminary simulations were conducted to determine the necessary domain dimensions, as a function of blade length. The presented domain dimensions are a result of this. Results regarding airflow characteristics (the specific analysis techniques are discussed in greater details in Section II-C) were found to be identical when the two blades were simulated to interact in a domain four times the size (upstream dimension increase from 1.2L to 2.4L, downstream dimension increase from 6L to 12L and side wall distance increase from 2L to 4L). Therefore, the domain size was minimised, whilst maintaining the domain characteristics that justify the assumption that side wall effects were negligible.

The blades were modelled as infinitesimally thin walls, such that t_{BL}=0. The blade clamps, which were used throughout the model validation process, were not included. It was of primary importance to understand the effects of ϕ variation, and therefore both domain simplifications were implemented to remove possible causes of variance in the resolved data.

A triangular mesh was implemented throughout the domain, to accommodate the moving boundaries and allow for skewing and re-meshing in the region close to the blade boundaries. A moderate mesh resolution was implemented, with a node spacing of $\frac{L}{62}$ in the near vicinity of the moving blade boundaries, enlarging to $\frac{L}{31}$ in the far field. For the domain defining the three-blade array with a neutrally positioned middle blade (U_D=0), a total of 57,580 elements existed at t=0. In preliminary work, a domain meshed as such was

compared to the same domain with far greater mesh resolution (230,388 elements) using each of the validation methods described in Section II-C. The greatest discrepancy between results, found during the vortex trajectory comparison, was 1.27% and therefore the reduced computational demand was preferred.

B. Blade Motion

Equation 3 was used to define the mode shape of each blade at maximum amplitude, with a calibration coefficient, C_{YM}, used to account for the 31mm blade length, as described in Equations 5 and 6. Transient motion was implemented through Equation 4, with D_c defined by Equation 7. The resonant frequency of the blades was maintained at 100Hz throughout the investigation. A variable coefficient was added to the sine function in Equation 4 to achieve different phases of oscillation where necessary.

$$C_{YM} = \frac{0.065}{L} \tag{5}$$

$$y_{L65} = y \cdot C_{YM} \tag{6}$$

$$D_c = \frac{A}{1.0054} \tag{7}$$

The y-coordinate of each node on the blade boundaries was also varied for each transient step to best approximate the motion of an oscillating cantilever beam. The method was derived through during preliminary investigation [50]. Each point was assumed to maintain a constant distance from the point y=0.32L, regardless of blade's progress through an oscillation cycle.

Each complete oscillation in the transient solution was described by 160 unique time steps. A total of 60 oscillation were desired, as deemed sufficient from preliminary work [50], and therefore 9600 time steps were resolved in total. Preliminary results revealed a skewed velocity profile if the blade boundary motion was immediately implemented to 100% of the desired amplitude. Peak amplitude was therefore built up in a linear manner over the initial 1600 time steps (referring to 10 completed blade oscillations).

C. Model Validation

The determined numerical model was validated against empirical findings documented by Kim *et al.* [32]. The validation procedure has been introduced in previously published literature [50]. Kim *et al.* reported experimental findings from apparatus that defined a flow domain as in Figure 3, where the side walls were 140.9 mm from either face of the blade and the blade was tightly confined at both edges. This had the effect of significantly reducing the blade edge effects observed during oscillation of an unconfined PE fan blade. Dimensionally, the blade itself was 31 mm × 38.1 mm × 0.13 mm ($L \times W \times t_{BL}$). It oscillated to an amplitude of 1.3716 mm, at a frequency of 180 Hz.

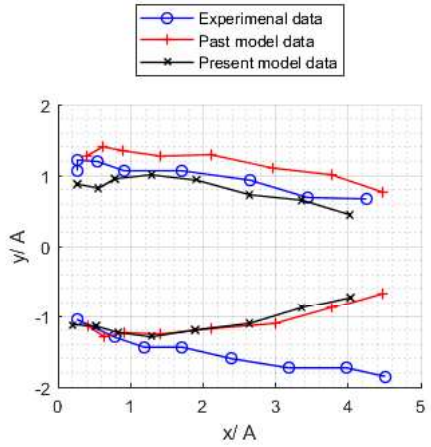

Fig. 8. The vortex trajectories outputted by the present model [50], compared with previous experimental data [32] and previous numerically modelled results [8]

Comparison of the generated downstream flow fields from a single fan blade defined the validation procedure. The modelled vortex size and trajectory were found to be well matched with experimental results. At $\frac{\pi}{4}$ and $\frac{\pi}{2}$ after vortex separation from the blade tip, vortex diameter error was 7.2% and 6.8% respectively. Averaged error, up to $\frac{3\pi}{2}$ after separation, was 11.5%. Vortex downstream trajectories are shown in Figure 8 [50]. The figure also includes the modelled vortex trajectories reported by Choi *et al.* [8]. Compared to the experimental results, the model used in the present investigation outputted a 10.6% (5.3%) error in the downstream displacement of the clockwise (counter-clockwise) vortex. Finally, modelled downstream volumetric flow rate was calculated, and found to have an error of 3.0% [50].

The small error observed across the range of comparative methods used for validation justifies the assumption that the inlet and outlet pressures are equal to a great extent. Should this assumption be invalid, the model would have outputted excessive downstream vortex trajectory rates, and over-approximated the generated volumetric flow rate. This is evidently not the case.

D. Investigatory Procedure

The blades' operational characteristics were maintained throughout the investigation. Amplitude was set to 3 mm and frequency to 100 Hz. Coupled with constant geometric characteristics, this prevented analysis of the controlled variable, ϕ, from being diluted by discrepancy due to variance in other areas. As the geometric constraints are dimensionally relative to the pitch and oscillation amplitude of the blade, analysis and conclusions from the present study may be applied to geometrically dissimilar systems.

The focus of the investigation was to understand the effect on the generated airflow when the phase difference

between two adjacent blades, ϕ, in a PE fan array. A two-blade array represents the simplest PE fan array, and performance characterisation and optimisation on such an array is established in the field since 1994 [9] [27] [51] [52] [53].

Phase difference in a simple two-blade array was varied from 0°(IP oscillation) to 180°(CP oscillation). A single array geometry was required to define the initial domain (Figure 7). Phase was varied from 0°to 180°in 15°increments, to create 13 sets of data in all.

Pitch has been the subject of prior investigations [50], which concluded it must be minimised to generate optimal airflow from an array of any given size. However, analysis also highlighted complex flow fields in the region between the two blades when pitch was small, P <4A. P=4A was determined to be optimal for this investigation. At this pitch, it is established that vortices are able to grow in the same broad manner as from an unconfined blade, but the vortices interact significantly, unlike at larger pitches [50].

III. Results and Discussion

Figures 9 and 10 presents the modelled velocity vector fields at the instance of the LH blade tip reaching the edge of it's oscillation envelope (θ=90°), for all trialled cases of ϕ. At ϕ=0°and 180°, the RH blade is instantaneously stationary at the LH and RH edge of its oscillation respectively. For all other cases, the RH blade has a positive x-velocity.

As a primary basis of performance, the time-averaged downstream velocity, v_y, profiles at y=2L were compiled. They are displayed for all trialled ϕ cases in Figure 11. The skewness of each velocity profile highlighted in Figure 12, which plots the maximum velocity, $v_{y,max}$ (peak of each dataset displayed in Figure 11).

The volume* of generated downstream airflow, $\dot{V}_y^*$, may be deduced from the velocity profiles by integrating the function defining the profile across the full x-range. As the domain is 2D, the volume* is presented as an area, and $\dot{V}_y^*$ is defined in terms of '$m^2.s^{-1}$'. Figure 13 displays $\dot{V}_y^*$ results against ϕ.

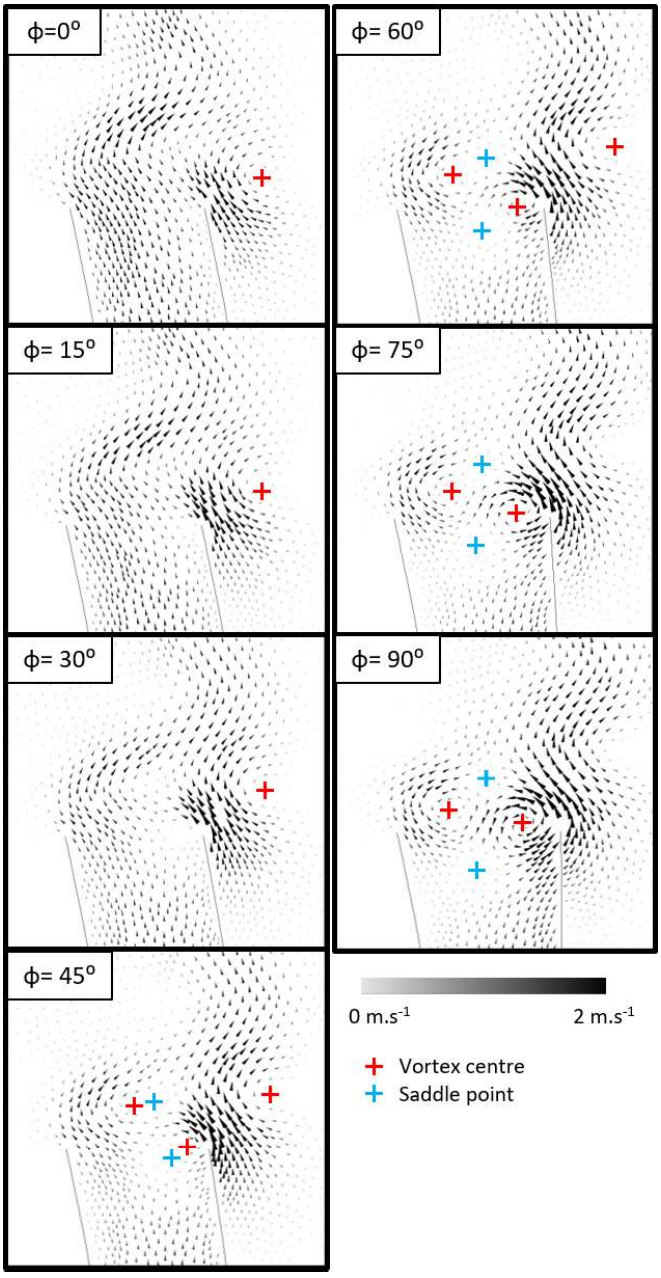

Fig. 9. Velocity vector fields at θ=90°, for $\phi \leq$90°

A. Optimal Performance

Figure 13 quantifies the qualitative hypotheses made: CP oscillation optimises a two-blade array in a channel flow application. CP oscillation of the present array generates 14.4% more airflow than IP oscillation. It is evident that IP oscillation is not the least optimal phase for a two-blade array, generating 3.4% more airflow than ϕ=60°.

Performance is highly dependent on vortex formation and growth at the blade tips, and the instances displayed in Figures 9 and 10 allow analysis of this phenomenon. Take first the IP case, where a single vortex is present in the considered region, formed on the trailing face of the RH blade. The nature of oscillation and the proximity of the adjacent blade means no vortex has been able to form behind the LH blade. Over the course of an oscillation cycle therefore, two vortices detach from the array with a downstream trajectory. This process has been documented in published literature [50], concluding that whilst a consistent downstream flow is generated over the course of the oscillation cycle, optimal $\dot{V}_y^*$ is not achieved.

In contrast, two well formed vortices are present in the CP case displayed in Figure 10, and a further two are formed on the outer faces of the blades during the closing period of array oscillation, detaching at the instance θ=270°. Therefore, a total of four vortices are projected downstream by the array during a single oscillation cycle. Published findings [28]

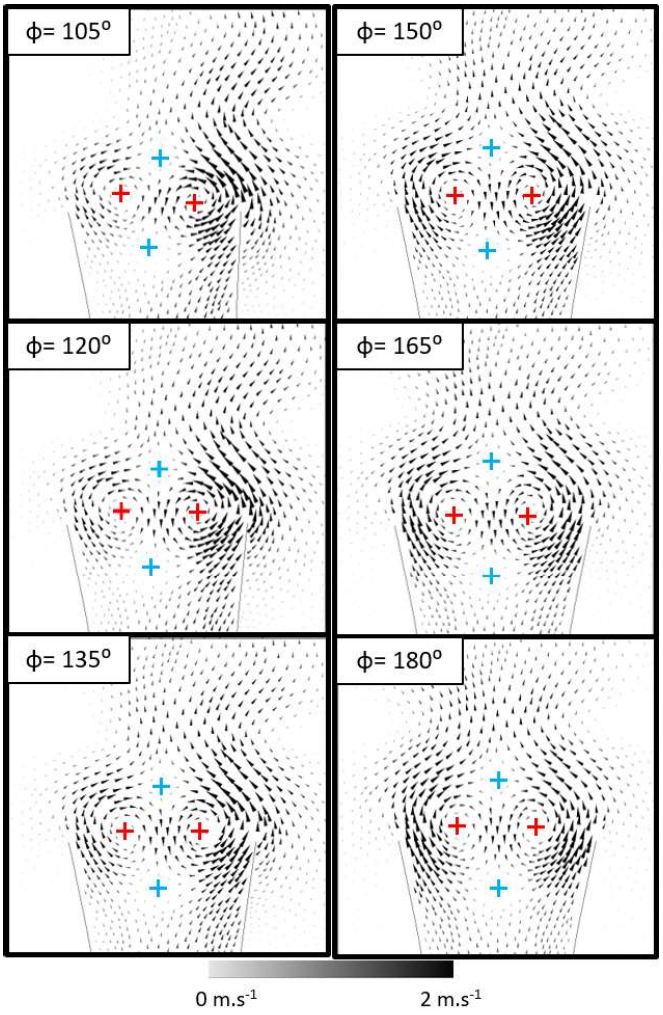

Fig. 10. Velocity vector fields at θ=90°, for ϕ >90°

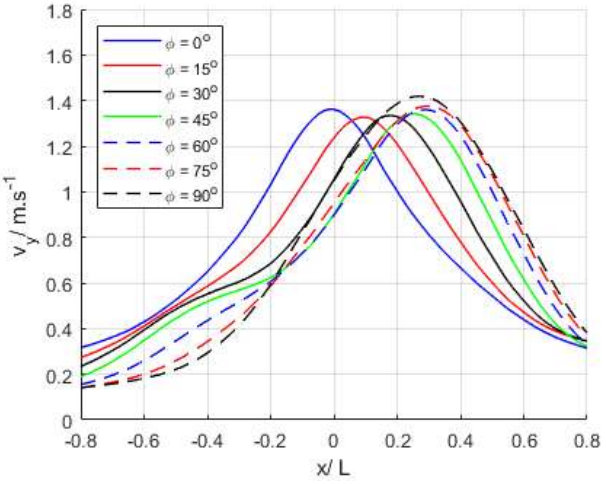

(a) $\phi \leq$90°cases

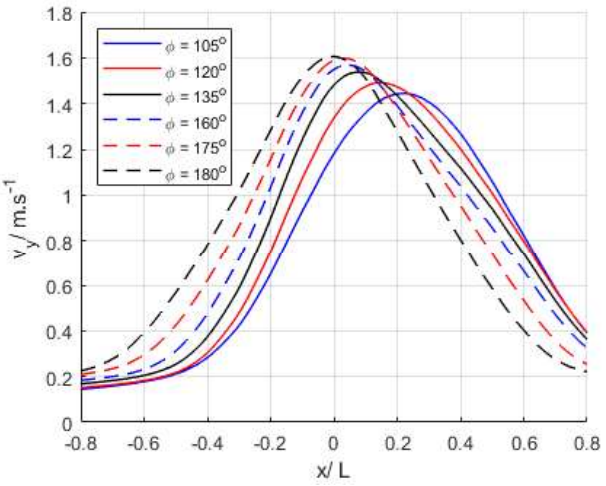

(b) ϕ >90°cases

Fig. 11. Time-averaged downstream velocity profiles at y=2L

have demonstrated how each vortex pair interacts to enhance performance, a phenomenon termed 'beneficial coupling', and this is plainly evident in the present investigation, with the aforementioned superior downstream airflow.

Optimal performance may also be considered in terms of the rate at which useful energy is added to the working fluid. Accordingly, Figure 14 plots the average rate of kinetic energy addition to the air for all considered ϕ values. The values are calculated assuming incompressible air with a density of 1.225 kg.m^{-2} and considering only airflow in the downstream direction. The left hand axis represents results for a normalised blade width of 1 m. The performance enhancement of CP oscillation is enhanced under this measure, the rate of useful energy addition to the working fluid is 49.6% greater, compared to IP oscillation. The right hand axis provides results more relevant for real world application, by considering a blade width of 25.4 mm.

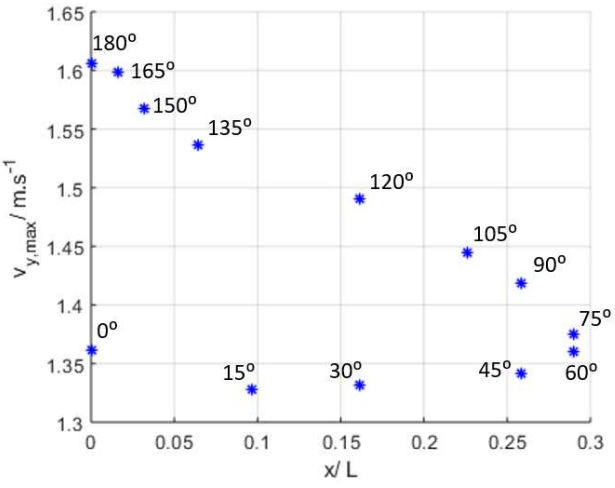

Fig. 12. x-location of $v_{y,max}$ for each ϕ case

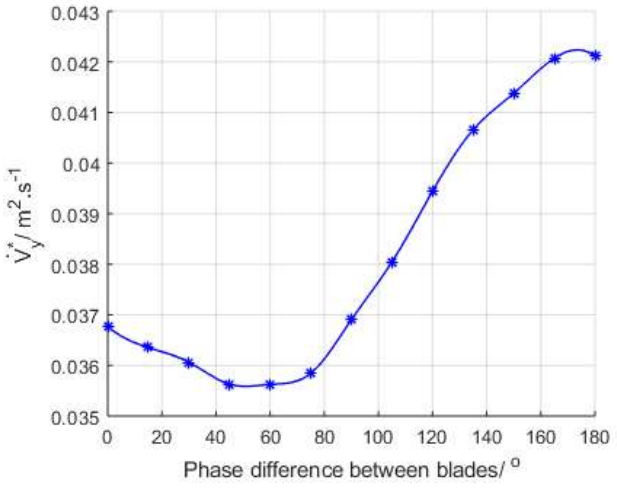

Fig. 13. Volume of downstream airflow at y=2L for each trialled phase

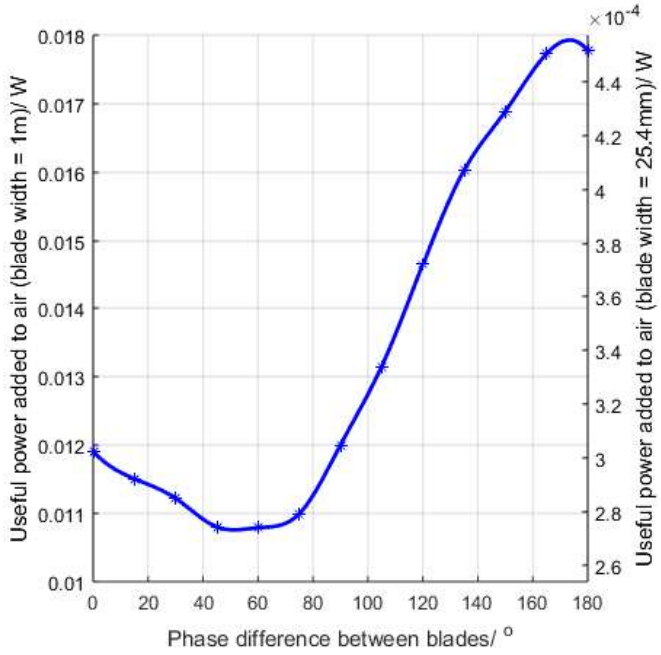

Fig. 14. Rate of useful energy addition to the air, for each trialled phase. The left hand axis provides data for a normalised blade width of 1 m, the right hand axis provides data for a blade width of 25.4mm

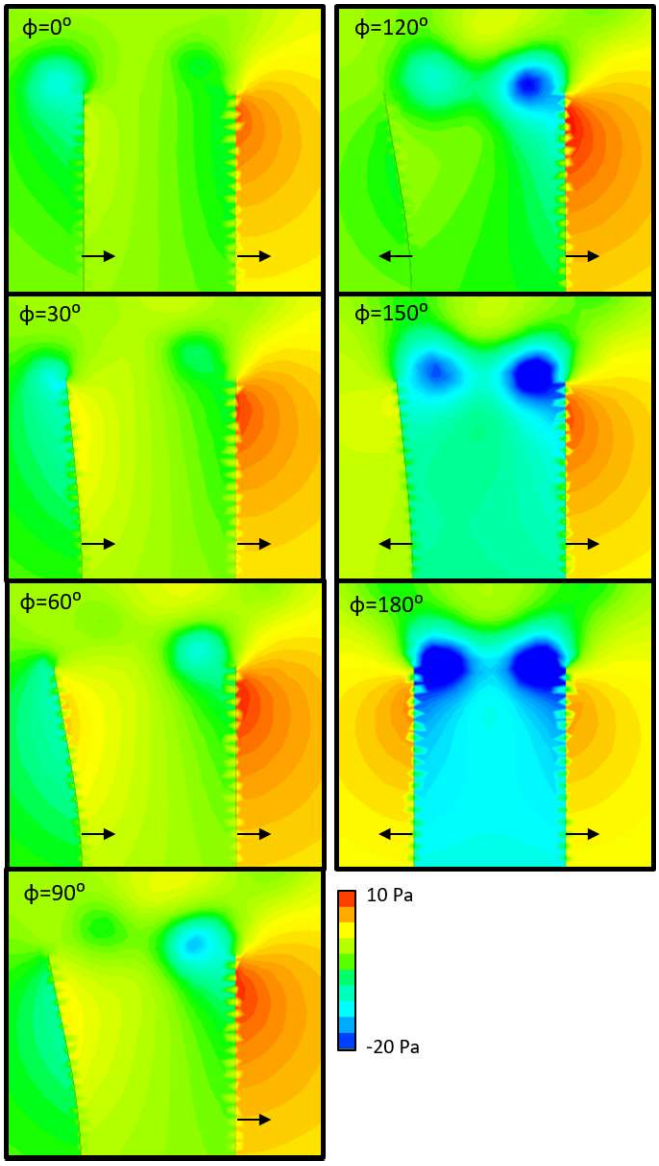

Fig. 15. Gauge pressure contour plots of the close field region at the instance the RH blade reaches oscillation centre with a positive x-velocity for the cases ϕ=0°, 30°, 60°, 90°, 120°, 150°and 180°

B. Phase Variation

Phase variation was identified as a possible means to induce skew in the generated downstream velocity profiles. This skew is evident in Figure 11. The skewness is substantial at its peak, and it is proposed that the phenomenon may be developed for application, to drive airflow in a direction misaligned with that identified as "downstream" in the present study. The causes for skew are investigated in this section.

The range of ϕ values trialled in the present investigation allow observation of two-blade array performance in an incremental format. Increasing from the ϕ=0°case, the requirement for a phase difference to allow vortex formation between the two blades is apparent. This is presented in Figure 15, pressure contour plots of the considered region at the instance the right hand blade reaches the centre of its oscillation envelope, moving with a positive x-velocity, for seven cases.

As ϕ increases, the area of low pressure behind the trailing face of the RH blade (around which the vortex is able to form) increases in both size and magnitude. A developed pressure gradient between the blades has been previously cited as a driver for enhanced downstream airflow [50]. Therefore it is interesting to note that, for the range $0°\leq \phi \leq 90°$, performance in terms of $\dot{V}_y^*$ varies by just 3.7%.

It may be hypothesised that the additional pressure gradient generated as ϕ is increased from 0°to 90°enhances velocity profile skewness, as displayed in Figure 11, rather than an increase in $\dot{V}_y^*$. Figure 12 provides evidence for this theory. ϕ increase from 0°to 60°drives significant skew: $v_{y,max}$ at ϕ=60°occurs at x=0.29$\frac{x}{L}$, but is detrimental to $\dot{V}_y^*$ magnitude. $\dot{V}_y^*$ improvement is only observed above this range, where skewness reduces with increasing ϕ. As skewness of the resolved velocity profile reduces, $\dot{V}_y^*$ performance is rapidly enhanced. For instance, assessing variation from ϕ=75°to ϕ=120°, skewness is reduced by 44.8% whilst $\dot{V}_y^*$ increases by 10.0%.

Variation in the velocity vector fields displayed in Figures 9 and 10 for ϕ=75°to ϕ=120°is the cause of the variation in the velocity profiles. Many comparable features are present: both contain two counter-rotating vortices and two saddle points, in similar alignment, between the blades and the volume of flow is weighted to the the $x >$0 region.

The fundamental difference between the two cases is not observable by observing a single θ instance. Increasing ϕ reduces the time between the initial formation of the LH and RH vortices, $\triangle\theta_{int}$. For ϕ=75°, the initiation of the LH and RH vortices occurs at θ=0°and θ=22°respectively, hence $\triangle\theta_{int,75}$=22°. For ϕ=120°, initiation occurs at θ=330°(equivalent θ=-30°) for the LH vortex and θ=342°(equivalent θ=-18°) for the RH vortex, and therefore $\triangle\theta_{int,120}$=12°. The y-position difference of the LH and RH vortex centres, $\triangle y_{vc}$, at any one instance is dependent on $\triangle\theta_{int}$, due to the method of vortex formation in the region confined by the two blades, and increases with it. Taking θ=90°, as in Figures 9 and 10, when ϕ=75°, $\triangle y_{vc}$=2.05mm, whilst for ϕ=120°, $\triangle y_{vc}$=0.47mm.

Relative vortex size and magnitude at a given instance is also dependent upon $\triangle\theta_{int}$. This is quantifiable by way of an example at θ=90°, the instance recorded in Figures 9 and 10. For ϕ=75°, maximum vorticity for the LH and RH vortices is υ_{max}=2006s^{-1} and υ_{max}=4033s^{-1} respectively and therefore the difference, $\triangle\upsilon_{max}$, is 2027s^{-1}. At ϕ=120°, υ_{max}=2270s^{-1} for the LH vortex and υ_{max}=3394s^{-1} for the RH vortex, hence $\triangle\upsilon_{max}$=1124s^{-1}.

The variance in $\triangle\theta_{int}$ and $\triangle y_{vc}$ may be referred to the published analysis presented regarding the vortex interaction displayed in Figure 5 [28], which is summarised in Section I-C. For large $\triangle\theta_{int}$ and $\triangle y_{vc}$ (at ϕ=75°), the RH vortex is able to dominate the LH vortex significantly and subsequently a large skew is induced in the downstream airflow. Increasing ϕ has the effect of reducing $\triangle\theta_{int}$. As a result, $\triangle y_{vc}$ at any given instance is also reduced. The reduction in $\triangle\theta_{int}$ and therefore in both $\triangle y_{vc}$ and $\triangle\upsilon_{max}$ affects vortex interaction. The evenly matched vortices generate significantly less skew in the downstream airflow, but the effect of beneficial coupling is enhanced and the volume of downstream airflow is improved.

The benefits of minimising $\triangle\theta_{int}$, and therefore $\triangle y_{vc}$ and $\triangle\upsilon_{max}$ too, are also demonstrated by comparing the ϕ=120°case with the ϕ=180°case. At θ=90°, for the ϕ=180°case, $\triangle\upsilon_{max}$=342s^{-1}, the minimum $\triangle\upsilon_{max}$ value for all cases trialled. Although $\triangle y_{vc}$=0.47mm for the former, apparently very small in the context of the entire domain, performance, in terms of $\dot{V}_y^*$, is enhanced by 6.72% as a result of eliminating $\triangle y_{vc}$ all together, achieved at ϕ=180°.

Furthering the evaluation of skewness's relationship with $\dot{V}_y^*$, it is evident that only 1.94% performance enhancement may be achieved by increasing ϕ from 150°to 180°(CP). Across the same range, skewness discrepancy is also small: 0.03$\frac{x}{L}$. It can be inferred, therefore, that away from IP oscillation (ϕ close to 0°), performance of an array may be evaluated simply by analysing the skew in the generated downstream velocity profile. By minimising skew in terms of $\frac{x}{L}$, optimisation of the two-blade array is achieved.

Comparing the ϕ=90°and ϕ=180°cases in Figures 9 and 10 respectively, many similarities can be observed in the flow field region between the two blades. Two counter-rotating vortices are present in both cases, and two saddle points also feature, positioned centrally between the vortices, one upstream and the other downstream. Performance is better interrupted from the pressure contour maps displayed in Figure 15. The LH blade is at a different point in it's oscillation cycle and direct comparison between the same two cases is therefore not possible by this measure. However, the RH blade is at the same point, and there is clear discrepancy in the size and magnitude of the region of low pressure behind it's trailing face. This observation is agreeable with previously established relationships that large pressure gradient between the adjacent blades is a key factor for optimising $\dot{V}_y^*$.

It is hypothesised that the increased pressure gradient is attributed to the rate of displacement increase, $\dot{s}_i$, between the adjacent blade tips. By optimising this, which is done so by establishing CP oscillation, $\dot{V}_y^*$ will be optimal for the array geometry in a channel flow scenario. To evaluate this remark, the maximum displacement increase rate, $\dot{s}_{i,max}$, during the oscillation cycle for each ϕ case trialled is plotted against $\dot{V}_y^*$ in Figure 16.

Parallels can be drawn between the dataset displayed in Figure 16 and previous analysis regarding skew. In the range 0°$\leq \phi \leq$75°, increased $\dot{s}_{i,max}$ is detrimental to $\dot{V}_y^*$ but, as discussed, induces increasing skew in the downstream velocity profile. In the range 75°$\leq \phi \leq$180°(where skew is reduced with increasing ϕ), $\dot{V}_y^*$ is shown to increase with $\dot{s}_{i,max}$ in close to linear proportion. The relationship between $\dot{V}_y^*$ and $\dot{s}_{i,max}$ is verified by comparing the cases ϕ=165°and ϕ=180°. There is a very small discrepancy in $\dot{s}_{i,max}$ between the two, 0.85%, and as a result comparable volume flow rates are imparted on the downstream region: varying by just 0.10%.

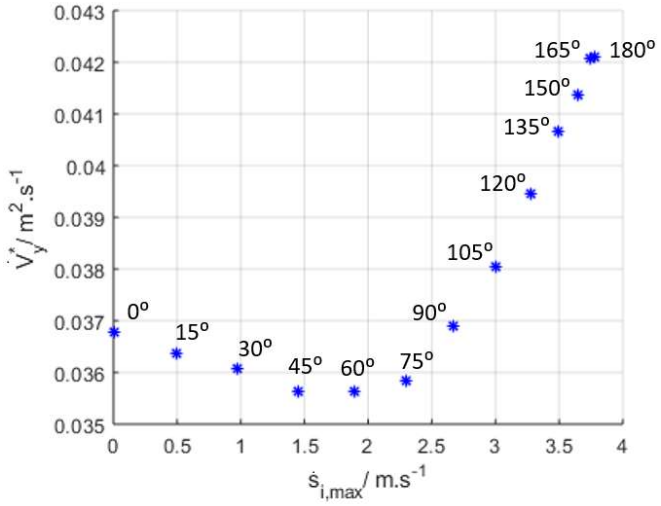

Fig. 16. Maximum rate of displacement increase between adjacent blade tips during an oscillation cycle plotted against volume* of downstream airflow for each ϕ case

IV. Conclusions

Phase variation away from IP (ϕ=0°) and CP (ϕ=180°) oscillation introduces an asymmetrical flow domain. Analysis considered the incremental increase of ϕ from 0°to 180°. Two high level phenomena were observed: skew increase when ϕ ≤60°and generated downstream airflow increase when ϕ ≥75°.

The analysis was conducted considering the unique channel flow scenario introduced in the investigation. Conclusions drawn may be assumed to be justified for any channel flow scenario, even with varying geometric or operational parameters.

At ϕ=60°, $v_{y,max}$ is found at x=0.29$\frac{x}{L}$, representing the greatest recorded skew. The skew in this instance is considerable, and may be used in industry application, where the direction of airflow must be varied to provide varying levels of cooling capability for different components within an assembly, once in operation.

Performance is worst at ϕ=60°, 3.4% poorer than at ϕ=0°. For ϕ=75°, skew remains at x=0.29$\frac{x}{L}$, but improved airflow generation performance is first observed. When ϕ ≥75°, airflow performance increases with ϕ, whilst skew reduces in approximately linear proportion to performance increase.

The generated skew is attributed to the dominance of one vortex over another in the region between two adjacent blades. For a highlighted instance of the ϕ=75°case (representing maximum skew), peak vorticity is 101% greater in the RH vortex. The discrepancy in vorticity magnitude between the LH and RH vortices reduces as ϕ is increased.

The maximum velocity of one blade tip relative to the other, $\dot{s}_{i,max}$, during oscillation of the two-blade FTF array is shown to be a characteristic through which performance may be established, when ϕ ≥75°and skew is no longer the dominant phenomenon. Maximised $\dot{s}_{i,max}$ is essential for optimal performance. This relationship may be applied to PE fan array research away from phase variation analysis as it is closely related to the generated pressure gradient between two adjacent FTF blades in an array.

Analysis of the results produced in the present investigation verify qualitative hypotheses made. In a channel flow application, optimal FTF array performance is achieved through CP oscillation of adjacent PE fan blades. Considering a measured downstream volume flow rate in the far field, CP oscillation outperformed IP oscillation by 14.4%.

It is assumed throughout this study that the inlet and outlet pressures were equal, a methodology established in the PE fan field. This assumption was validated against published empirical data for the model used in the present investigation, to a reasonable degree of error.

Acknowledgements

The authors would like to acknowledge the support of the UK Engineering and Physical Sciences Research Council (EPSRC) under the project grant EP/P030157/1.

References

[1] M. Toda, "Theory of air flow generation by a resonant type PVF2 bimorph cantilever vibrator," pp. 911–918, 1978.
[2] A. Hales and X. Jiang, "A Review of Piezoelectric Fans for Low Energy Cooling of Power Electronics," *Applied Energy*, vol. 215, pp. 321–337, 2018.
[3] S. Liu, R. Huang, W. Sheu, and C. Wang, "Heat transfer by a piezoelectric fan on a flat surface subject to the influence of horizontal/vertical arrangement," *International Journal of Heat and Mass Transfer*, vol. 52, pp. 2565–2570, 2009.
[4] J. H. Yoo, J. I. Hong, and W. Cao, "Piezoelectric ceramic bimorph coupled to thin metal plate as cooling fan for electronic devices," *Sensors and Actuators*, vol. 79, no. 1, pp. 8–12, 2000.
[5] H. H. Kolm and E. A. Kolm, "Solid state blower," 1985.
[6] N. Jeffers, K. P. Nolan, J. Stafford, and B. Donnelly, "High fidelity phase locked PIV measurements analysing the flow fields surrounding an oscillating piezoelectric fan," *Journal of Physics: Conference Series*, vol. 525, pp. 1–9, 2014.
[7] M. L. Kimber and S. V. Garimella, "Measurement and prediction of the cooling characteristics of a generalized vibrating piezoelectric fan," *International Journal of Heat and Mass Transfer*, vol. 52, no. 19-20, pp. 4470–4478, 2009.
[8] M. Choi, C. Cierpka, and Y. H. Kim, "Vortex formation by a vibrating cantilever," *Journal of Fluids and Structures*, vol. 31, pp. 67–78, 2012.
[9] A. Ihara and H. Watanabe, "On the flow around flexible plates, oscillating with large amplitude," *Journal of Fluids and Structures*, vol. 8, pp. 601–619, 1994.
[10] C. Lin, "Analysis of three-dimensional heat and fluid flow induced by piezoelectric fan," *International Journal of Heat and Mass Transfer*, vol. 55, pp. 3043–3053, 2012.
[11] M. Hajmohammadi and I. Toghraei, "Optimal design and thermal performance improvement of a double-layered microchannel heat sink by introducing al2o3 nano-particles into the water," *Physica A: Statistical Mechanics and its Applications*, vol. 505, pp. 328 – 344, 2018. [Online]. Available: http://www.sciencedirect.com/science/article/pii/S0378437118303601
[12] T. Acikalin and S. V. Garimella, "Analysis and Prediction of the Thermal Performance of Piezoelectrically Actuated Fans," *Heat Transfer Engineering*, vol. 30, no. 6, pp. 487–498, 2009.

[13] M. L. Kimber, K. Suzuki, N. Kitsunai, K. Seki, and S. V. Garimella, "Pressure and flow rate performance of piezoelectric fans," *IEEE Transactions on Components and Packaging Technologies*, vol. 32, no. 4, pp. 766–775, 2009.

[14] C. S. Sharma, G. Schlottig, T. Brunschwiler, M. K. Tiwari, B. Michel, and D. Poulikakos, "Energy efficient hotspot-targeted embedded liquid cooling for electronics: An experimental study," *International Journal of Heat and Mass Transfer*, vol. 88, pp. 684–694, 2015.

[15] M. Hajmohammadi, M. Ahmadian, and S. Nourazar, "Introducing highly conductive materials into a fin for increasing the heat transfer enhancement," *International Journal of Mechanical Sciences*, vol. 150, 10 2018.

[16] M. Hajmohammadi and E. Rezaei, "Proposing a new algorithm for the optimization of conduction pathways based on a recursive localization," *Applied Thermal Engineering*, vol. 151, pp. 146 – 153, 2019. [Online]. Available: http://www.sciencedirect.com/science/article/pii/S1359431118361933

[17] J. G. Koomey, "Worldwide electricity used in data centers," *Environmental Research Letters*, vol. 3, no. 3, p. 034008, 2008.

[18] ——, "Growth in data center electricity use 2005 to 2010," *Analytical Press*, 2011.

[19] S. V. Garimella, T. Persoons, J. Weibel, and L. T. Yeh, "Technological drivers in data centers and telecom systems: Multiscale thermal, electrical, and energy management," *Applied Energy*, vol. 107, pp. 66–80, 2013.

[20] A. H. Khalaj and S. K. Halgamuge, "A Review on efficient thermal management of air- and liquid-cooled data centers: From chip to the cooling system," *Applied Energy*, vol. 205, no. March, pp. 1165–1188, 2017.

[21] L. Newborough, M. Newborough, and S. Probert, "Electronically commutated direct-current motor for driving tube-axial fans: A cost-effective design," *Applied Energy*, vol. 36, no. 3, pp. 167–190, jan 1990.

[22] M. L. Kimber, R. Lonergan, and S. V. Garimella, "Experimental study of aerodynamic damping in arrays of vibrating cantilevers," *Journal of Fluids and Structures*, vol. 25, no. 8, pp. 1334–1347, 2009.

[23] H. K. Ma, H. C. Su, and W. F. Luo, "Investigation of a piezoelectric fan cooling system with multiple magnetic fans," *Sensors and Actuators A: Physical*, vol. 189, pp. 356–363, 2013.

[24] H. K. Ma, Y. T. Li, and C. P. Lin, "Study of a dual-sided multiple fans system with a piezoelectric actuator," *Journal of Thermal Science*, vol. 24, no. 5, pp. 432–441, 2015.

[25] M. Choi, C. Cierpka, and Y. H. Kim, "Effects of the distance between a vibrating cantilever pair," *European Journal of Mechanics B/Fluids*, vol. 43, pp. 154–165, 2014.

[26] S. F. Sufian, Z. M. Fairuz, M. Zubair, M. Z. Abdullah, and J. J. Mohamed, "Thermal analysis of dual piezoelectric fans for cooling multi-LED packages," *Microelectronics Reliability*, vol. 54, no. 8, pp. 1534–1543, 2014.

[27] M. L. Kimber, S. V. Garimella, and A. Raman, "An experimental study of fluidic coupling between multiple piezoelectric fans," in *Thermomechanical Phenomena in Electronic Systems*, 2006, pp. 333–340.

[28] M. Choi, S. Y. Lee, and Y. H. Kim, "On the flow around a vibrating cantilever pair with different phase angles," *European Journal of Mechanics B/Fluids*, vol. 34, pp. 146–157, 2012.

[29] S. F. Sufian, M. Z. Abdullah, and J. J. Mohamed, "Effect of synchronized piezoelectric fans on microelectronic cooling performance," *International Communications in Heat and Mass Transfer*, vol. 43, pp. 81–89, 2013.

[30] R. Phillips and C. W. Dunnill, "Zero gap alkaline electrolysis cell design for renewable energy storage as hydrogen gas," *RSC Adv.*, vol. 6, no. 102, pp. 100 643–100 651, 2016. [Online]. Available: http://xlink.rsc.org/?DOI=C6RA22242K

[31] M. Hajmohammadi, P. Alipour, and H. Parsa, "Microfluidic effects on the heat transfer enhancement and optimal design of microchannels heat sinks," *International Journal of Heat and Mass Transfer*, vol. 126, pp. 808 – 815, 2018. [Online]. Available: http://www.sciencedirect.com/science/article/pii/S0017931018309669

[32] Y. H. Kim, S. T. Wereley, and C. H. Chun, "Phase-resolved flow field produced by a vibrating cantilever plate between two endplates," *Physics of Fluids*, vol. 16, no. 1, pp. 145–162, 2004.

[33] A. Eastman and M. L. Kimber, "Flow shaping and thrust enhancement of sidewall bounded oscillating cantilevers," *International Journal of Heat and Fluid Flow*, vol. 48, pp. 35–42, 2014.

[34] ——, "Aerodynamic damping of sidewall bounded oscillating cantilevers," *Journal of Fluids and Structures*, vol. 51, pp. 148–160, 2014.

[35] J. Stafford and N. Jeffers, "Aerodynamic performance of a vibrating piezoelectric fan under varied operational conditions," *IEEE Transactions on Components, Packaging and Manufacturing Technology*, pp. 1–11, 2014.

[36] A. Almoli, A. Thompson, N. Kapur, J. Summers, H. Thompson, and G. Hannah, "Computational fluid dynamic investigation of liquid rack cooling in data centres," *Applied Energy*, vol. 89, no. 1, pp. 150–155, 2012.

[37] S. F. Sufian and M. Z. Abdullah, "Heat transfer enhancement of LEDs with a combination of piezoelectric fans and a heat sink," *Microelectronics Reliability*, vol. 68, pp. 39–50, 2017.

[38] X. Li, J. Zhang, and X. Tan, "Convective heat transfer on a flat surface induced by a vertically oriented piezoelectric fan in the presence of cross flow," *Heat Mass Transfer*, 2017.

[39] L. K. Tan, J. Zhang, and X. Tan, "Numerical investigation of convective heat transfer on a vertical surface due to resonating cantilever beam," *International Journal of Thermal Sciences*, vol. 80, pp. 93–107, 2014.

[40] T. Acikalin, A. Raman, and S. V. Garimella, "Two-dimensional streaming flows induced by resonating, thin beams," *The Journal of the Acoustical Society of America*, vol. 114, no. 4, pp. 1785–1795, 2003.

[41] M. K. Abdullah, M. Z. Abdullah, M. V. Ramana, C. Y. Khor, K. A. Ahmad, M. A. Mujeebu, Y. Ooi, and Z. Mohd Ripin, "Numerical and experimental investigations on effect of fan height on the performance of piezoelectric fan in microelectronic cooling," *International Communications in Heat and Mass Transfer*, vol. 36, no. 1, pp. 51–58, 2009.

[42] M. K. Abdullah, M. Z. Abdullah, S. F. Wong, C. Y. Khor, Y. Ooi, K. A. Ahmad, Z. M. Ripin, and M. A. Mujeebu, "Effect of piezoelectric fan height on flow and heat transfer for electronics cooling applications," in *10th International Conference on Electronic Materials and Packaging*, 2008, pp. 165–170.

[43] S. F. Sufian, M. Z. Abdullah, M. K. Abdullah, and J. J. Mohamed, "Effect of side and tip gaps of a piezoelectric fan on microelectronic cooling," *IEEE Transactions on Components, Packaging and Manufacturing Technology*, vol. 3, no. 9, pp. 1545–1553, 2013.

[44] M. K. Abdullah, N. C. Ismail, M. Abdul Mujeebu, M. Z. Abdullah, K. A. Ahmad, M. Husaini, and M. N. A. Hamid, "Optimum tip gap and orientation of multi-piezofan for heat transfer enhancement of finned heat sink in microelectronic cooling," *International Journal of Heat and Mass Transfer*, vol. 55, no. 21-22, pp. 5514–5525, 2012.

[45] Z. M. Fairuz, S. F. Sufian, M. Z. Abdullah, M. Zubair, and M. S. Abdul Aziz, "Effect of piezoelectric fan mode shape on the heat transfer characteristics," *International Communications in Heat and Mass Transfer*, vol. 52, pp. 140–151, 2014.

[46] M. A. Bidakhvidi, S. Vanlanduit, R. Shirzadeh, and D. Vucinic, "Experimental and computational analysis of the flow induced by a piezoelectric fan," in *15th International Symposium on Flow Visualisation*, 2012.

[47] B. E. Launder and D. B. Spalding, "The Numerical Computation of Turbulent Flows," *Computer Methods in Applied Mechanics and Engineering*, vol. 3, no. 2, pp. 269–289, 1974.

[48] L. Meirovitch, *Analytical Methods in Vibrations*. London: Collier-MacMillan Ltd., 1967.

[49] L. A. Florio and A. Harnoy, "Use of a vibrating plate to enhance natural convection cooling of a discrete heat source in a vertical channel," *Applied Thermal Engineering*, vol. 27, no. 13, pp. 2276–2293, 2007.

[50] A. Hales and X. Jiang, "Geometric optimisation of piezoelectric fan arrays for low energy cooling," *International Journal of Heat and Mass Transfer*, vol. 137, pp. 52–63.

[51] M. L. Kimber and S. V. Garimella, "Cooling performance of arrays of vibrating cantilevers," *Journal of Heat Transfer*, vol. 131, no. 11, pp. 1–8, 2009.

[52] T. Acikalin, S. M. Wait, S. V. Garimella, and A. Raman, "Experimental investigation of the thermal performance of piezoelectric fans," *Heat Transfer Engineering*, vol. 25, no. 1, pp. 4–14, 2004.

[53] R. R. Schmidt, "Local and average transfer coefficients on a vertical surface due to convection from a piezoelectric fan," in *Intersociety Conference on Thermal Phenomena in Electronic Systems*, 1994, pp. 41–49.

Alastair Hales received an M.Eng degree in mechanical engineering from the University of Bristol, UK in 2012 and a Ph.D degree in mechanical engineering from the University of Bristol, UK in 2016.

He is a Research Associate with the Faculty of Engineering at Imperial College, London. His current research is focussed on the thermal management of lithium-ion cells. Previously, he has worked on the development and optimisation of alternative air-mover technology for low energy cooling of power electronics.

Xi Jiang is a Professor of Mechanical Engineering at Queen Mary University of London. He has an academic profile previously developed at Brunel University, Queen Mary University of London, Building Research Establishment, Seoul National University and University of Science and Technology of China. His research has been in the broad area of Energy and Environments. He is the principal investigator in several current research projects, one of which is focussed on the development and optimisation of alternative air-mover technology for the cooling of power electronics.

Professor Jiang was the winner of the Gaydon Prize for the most significant UK contribution to the 28th Symposium (International) on Combustion by the Combustion Institute. He has also been involved in organizing international conferences in energy utilisation and multi-phase flows.

Conflict of Interest

The authors, Dr. Alastair Hales and Prof. Xi Jiang, confirm that there is no conflict of interest surrounding the findings in this manuscript.